

Unusual Reactivity of a Cr₂P₂ Tetrahedral Complex toward Superhydride; Formation of [CpCr(CO)₂]₂(μ-PH)₂(μ-H)_{2-x} (x = 1 and 2) and [CpCr(CO)₂]₂(μ-PH){(CpCr)₂(μ,η¹:η¹:η⁵:η⁵-P₅)}†

Perumal Sekar,[‡] Manfred Scheer,^{*,‡} Andreas Voigt,[§] and Reinhard Kirmse[§]

Institut für Anorganische Chemie, Universität Karlsruhe, D-76128 Karlsruhe, Germany, and Institut für Anorganische Chemie, Universität Leipzig, Talstrasse 35, D-04103 Leipzig, Germany

Received February 16, 1999

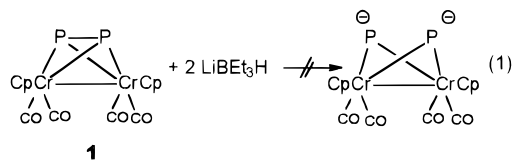
Reaction of [CpCr(CO)₂]₂(μ,η²-P₂) (**1**) with LiBEt₃H in THF at -78 °C affords the new phosphanido complexes [CpCr(CO)₂]₂(μ-PH)₂(μ-H) (**2**), [CpCr(CO)₂]₂(μ-PH)₂ (**3**), and [CpCr(CO)₂]₂(μ-PH){(CpCr)₂(μ,η¹:η¹:η⁵:η⁵-P₅)} (**4**), which have been characterized by single-crystal X-ray diffraction methods. The structure of **4** reveals a triple-decker sandwich complex with a distorted cyclo-P₅ middle deck. The EPR spectrum of the paramagnetic (*S* = 1/2) complex **4** (*T* = 130 K) is interpreted with a rhombic-symmetric spin Hamiltonian. A noticeable hyperfine interaction with two ³¹P nuclei is observed.

Introduction

The research area of complexes with “naked” E_{*n*} ligands (E = P, As, Sb, Bi) has undergone a dynamic and exciting development.¹ Although the isolobal relationship between the fragments E and CH exists, the E_{*n*} units possess additional lone pairs in comparison to (CH)_{*n*}-ligands, which lead to many more structural manifolds of the formed coordination polyhedrons. The majority of publications in this area deals with the synthesis and structural features of such E_{*n*}-containing complexes. However, only during the past few years has the investigation of their reaction behaviors, especially those of P_{*n*} ligand complexes, been started by our group² and by the groups of M. Di Vaira,³ O. J. Scherer,⁴ and M. Mays.⁵

In one of our projects in this field, we are interested in synthesizing transition metal linked oligomers and polymers from P_{*n*} ligand complexes. For this purpose it

is necessary to have (i) suitable starting materials that are (ii) obtainable in good yields. The latter is a general problem in this synthetic field.¹ The synthesis of the complex [CpCr(CO)₂]₂(μ,η²-P₂) (**1**), obtained in 53% yield, was reported by Goh et al.⁶ Starting from this complex, we tried first to cleave its P–P bond by using superhydride to generate a dianionic complex according to eq 1. Although this reaction pattern is known for



disulfur complexes (e.g., [Fe₂(CO)₆(μ-S₂)]),⁷ complex **1** undergoes unexpected transformation pathways. The results are reported herein.

Results and Discussion

The reaction of **1** with 2 equiv⁸ of LiBEt₃H at -78 °C results in the isolation of the novel PH-containing complexes **2–4** (eq 2). Separation of the products by column chromatography leads to pure **2** as the main product of the reaction, whereas **3** and **4** were obtained only as a mixture, from which they crystallized side-by-side. They are green (**2**), orange (**3**), and dark brown (**4**) air-sensitive complexes, which are slightly soluble in hexane but readily soluble in toluene, CH₂Cl₂, and THF. Although they are stable in the solid state and complex **2** is stable in solution under an inert atmo-

† Dedicated to Professor R. Schmutzler on the occasion of his 65th birthday.

[‡] Universität Karlsruhe.

[§] Universität Leipzig.

(1) Reviews: (a) Scheer, M.; Herrmann, E. *Z. Chem.* **1990**, *29*, 41. (b) Scherer, O. J. *Angew. Chem., Int. Ed. Engl.* **1990**, *29*, 1104. (c) Di Vaira, M.; Stoppioni, P. *Coord. Chem. Rev.* **1992**, *120*, 259.

(2) (a) Scheer, M.; Dargatz, M.; Jones, P. G. *J. Organomet. Chem.* **1993**, *447*, 259. (b) Scheer, M.; Becker, U. *Phosphorus, Sulfur Silicon Relat. Elem.* **1994**, *93–94*, 257.

(3) (a) Di Vaira, M.; Stoppioni, P.; Peruzzini, M., *J. Chem. Soc., Dalton Trans.* **1990**, 109. (b) Di Vaira, M.; Rovai, D.; Stoppioni, P. *Polyhedron* **1990**, *20*, 2477. (c) Di Vaira, M.; Stoppioni, P.; Laschi, F.; Zanello, P. *Polyhedron* **1991**, *10*, 2123.

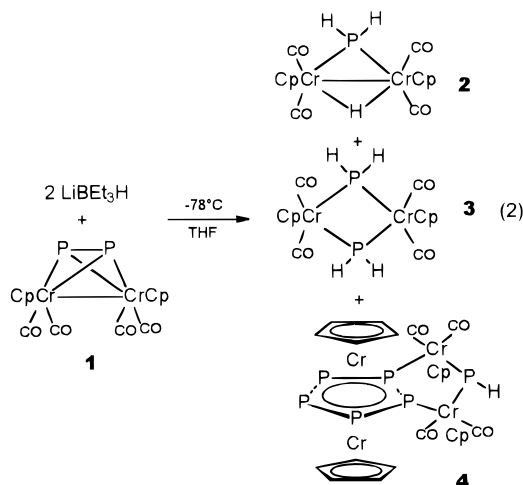
(4) (a) Scherer, O. J.; Berg, G.; Wolmershäuser, G. *Chem. Ber.* **1995**, *128*, 635. (b) Detzel, M.; Mohr, T.; Scherer, O. J.; Wolmershäuser, G. *Angew. Chem., Int. Ed. Engl.* **1994**, *33*, 110. (c) Detzel, M.; Friedrich, G.; Scherer, O. J.; Wolmershäuser, G. *Angew. Chem., Int. Ed. Engl.* **1995**, *34*, 1321. (d) Scherer, O. J.; Weigel, S.; Wolmershäuser, G. *Chem. Eur. J.* **1998**, *4*, 1910.

(5) (a) Davies, J. E.; Mays, M. J.; Raitby, P. R.; Shields, G. P.; Tompkin, P. K. *J. Chem. Soc. Chem. Commun.* **1997**, 361. (b) Davies, J. E.; Kerr, L. C.; Mays, M. J.; Raitby, P. R.; Tompkin, P. K.; Woods, A. D. *Angew. Chem., Int. Ed. Engl.* **1998**, *37*, 1428. (c) Davies, J. E.; Klunduk, M. C.; Mays, M. J.; Raitby, P. R.; Shields, G. P.; Tompkin, P. K. *J. Chem. Soc., Dalton Trans.* **1997**, 715.

(6) Goh, L. Y.; Chu, C. K.; Wong, R. C. S.; Hambley, T. W. *J. Chem. Soc., Dalton Trans.* **1989**, 1951.

(7) Seyferth, D.; Henderson, R. S.; Song, Li.-C. *Organometallics* **1982**, *1*, 125.

(8) The use of a further excess of LiBEt₃H results in a quantitative yield of **2**. The source of the H atoms in the products is uncertain. The protolysis is completed by the column chromatography using deactivated Silcagel.



sphere, **3** and **4** slowly decompose in solutions of THF and CH_2Cl_2 . All products reveal molecular ion peaks in the mass spectra with the exception of **4**, for which the highest fragment is $[\text{M}^+ - 2\text{CO}]$.

The infrared spectrum of **2** displays a CO stretching pattern similar to that of the recently reported compound $[\text{Mo}_2\text{Cp}_2(\text{CO})_4(\mu\text{-PH}_2)(\mu\text{-H})]$, obtained from the reaction of $[\text{Mo}_2\text{Cp}_2(\text{CO})_4(\mu, \eta^2\text{-P}_2)]$ with M^iOH ($\text{M}^i = \text{Na}, \text{K}$) and subsequent HBF_4 addition.^{5a} The ^1H NMR spectrum of **2** shows a doublet of doublet centered at δ 5.1 for the PH_2 protons, revealing the couplings with the phosphorus atom and the bridging hydrogen atoms ($^1J_{\text{HP}} = 337$, $^3J_{\text{HH}} = 1.5$ Hz). The signal for the hydride bridging the Cr atoms occurs at δ -14.4 as a doublet ($^2J_{\text{PH}} = 75$ Hz). The ^{31}P NMR spectrum of **2** exhibits a doublet of triplet at δ 110.5 ($^1J_{\text{PH}} = 337$, $^2J_{\text{PH}} = 75$ Hz), revealing the coupling with both protons attached to it, as well as to the hydrogen atom bridging the Cr atoms. The ^{31}P NMR spectrum of **3** shows a triplet of triplet centered at δ -147.2 due to the coupling of the P atoms to the protons in different ways ($^1J_{\text{PH}} = 177$, $^3J_{\text{PH}} = 117$ Hz). The chemical shift appears upfield with respect to the complexes **1** and **2**. For the paramagnetic complex **4**, no NMR resonances could be detected.

The structures of **2–4** were established by single-crystal X-ray diffraction. The structure of **2** (Figure 1) consists of a planar Cr_2HP fragment, which is similar to Mays's molybdenum analogue.^{5a} However, only by comparison of their unit cell dimensions is it revealed that they are not isostructural. The crystal structure of **3** reveals three independent molecules, in which each of the two chromium atoms are bridged by two PH_2 groups in a symmetrical fashion. The bond parameters are similar, and they differ only in the folding angle of the butterfly Cr_2P_2 framework [molecule A: $152.92(9)^\circ$; B: $149.77(5)^\circ$; C: $157.94(4)^\circ$]. Figure 2 shows the molecular structure of molecule A. Although the Cr–Cr distance in **2** can be assigned as a slightly elongated single bond (3.104(1) Å) in comparison to those of **1** (3.011(1) Å) and $[(\text{CO})_4\text{CrP}(\text{CH}_3)_2]_2$ (2.950 Å),⁹ the distance in **3** (3.881 Å) falls beyond the range of a bond. The average Cr–P bond distance in **2** (2.269 Å) is slightly shorter than the average bond distances in **3** (2.381 Å, average distances of three independent molecules), **1** (2.409 Å),⁶ $[\text{Cp}_2\text{Cr}_2(\text{CO})_4(\mu, \eta^2\text{-P}_2)\{\text{Cr}(\text{CO})_5\}]$

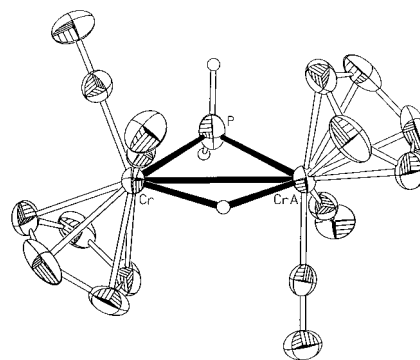


Figure 1. Molecular structure of **2** (ellipsoids drawn at of 50% probability level, H atoms of the Cp ligands are omitted for clarity). Selected bond lengths [Å] and angles [deg]: Cr–Cr(A) 3.104(1), Cr–P 2.2657(10), Cr(A)–P 2.2714(10), Cr–P–Cr(A) 86.34(3), P–Cr–Cr(A) 46.94(3), P–Cr(A)–Cr 46.79(3).

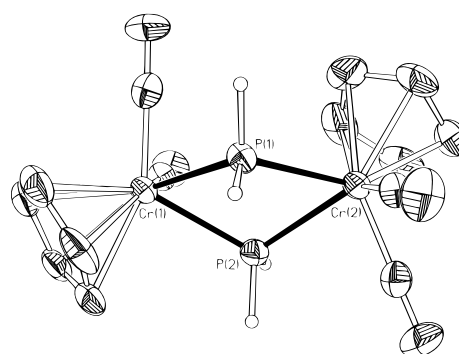


Figure 2. Molecular structure of **3** (molecule A; ellipsoids drawn at of 50% probability level, H atoms of the Cp ligands are omitted for clarity). Selected bond lengths [Å] and angles [deg]: Cr(1)–P(1) 2.383(2), Cr(1)–P(2) 2.384(2), Cr(2)–P(1) 2.382(2), Cr(2)–P(2) 2.377(2), Cr(2)–P(1)–Cr(1) 108.82(6), Cr(2)–P(2)–Cr(1) 108.98(6), P(1)–Cr(1)–P(2) 66.32(5), P(2)–Cr(2)–P(1) 66.43(5).

(2.405 Å),¹⁰ $[\text{Cp}_2\text{Cr}_2(\text{CO})_4(\mu, \eta^2\text{-P}_2)\{\text{Cr}(\text{CO})_5\}_2]$ (2.411 Å)¹¹ and in $[(\text{CO})_4\text{CrP}(\text{CH}_3)_2]_2$ (2.318 Å).⁹ Each chromium atom in **2** and **3** achieves the 18-electron configuration.

The molecular structure of **4** (Figure 3) displays a triple-decker sandwich with a pseudo-cyclo- P_5 middle deck, from which two of the P atoms coordinate to the Cr centers of the $[\{\text{CpCr}(\text{CO})_2\}_2(\mu\text{-PH})]$ moiety. The P–P distances in the P_5 middle deck vary between 2.103(5) and 2.315(5) Å for the shorter and between 2.455(5) and 2.490(6) Å for the longer ones, suggesting a partitioning of the P_5 ring in an allylic P_3 ¹² and a P_2 subunit (Figure 4). While the P–P single bond distance is 2.21 Å¹³ the longest so far still considered a P–P bond is 2.4616(22) Å in $[(\text{R}_3\text{P})_2\text{Rh}(\eta^2\text{-P}_4)\text{Cl}]$.¹⁴ This kind of distortion is unusual for the cyclo- P_5 middle deck in the triple-decker complexes $[(\text{Cp}^*\text{Cr})_2(\mu, \eta^{5.5}\text{-P}_5)]$ ¹⁵ and $[(\text{Cp}^*\text{Cr})_2(\mu, \eta^{5.5}\text{-P}_5)]$.

(10) Goh, L. Y.; Wong, R. C. S.; Mak, T. C. W. *J. Organomet. Chem.* **1989**, 373, 71.

(11) Goh, L. Y.; Wong, R. C. S.; Mak, T. C. W. *J. Organomet. Chem.* **1989**, 364, 363.

(12) exactly considered the P–P bond distances revealing a localized P–P double bond between atoms P3 and P4, while between P3 and P2 an elongated P–P single bond is determined.

(13) Simon, A.; Borrmann, H.; Horakh, J. *Chem. Ber./Recueil* **1997**, 130, 1235.

(14) Ginsberg, P.; Lindsell, W. E.; McCullough, K. J.; Sprinkle, C. R.; Welch, A. J. *J. Am. Chem. Soc.* **1986**, 108, 403.

(15) Scherer, O. J.; Schwalb, J.; Wolmershäuser, G.; Kaim, W.; Gross, R. *Angew. Chem., Int. Ed. Engl.* **1986**, 4, 363.

(9) Vahrenkamp, H. *Chem. Ber.* **1978**, 111, 3472.

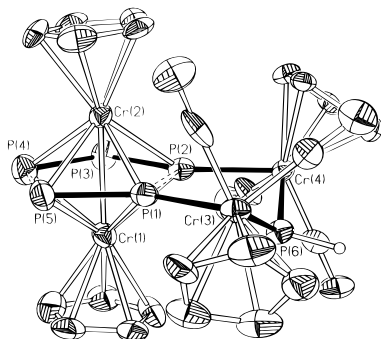


Figure 3. Molecular structure of **4** (ellipsoids drawn at of 50% probability level, H atoms of the Cp ligands are omitted for clarity). Selected bond lengths [Å] and angles [deg]: Cr(3)–P(1) 2.404(4), Cr(3)–P(6) 2.437(5), Cr(4)–P(2) 2.328(4), Cr(4)–P(6) 2.462(4), P(1)–P(2) 2.455(5), P(1)–P(5) 2.103(5), P(2)–P(3) 2.315(5), P(3)–P(4) 2.146(6), P(4)–P(5) 2.490(6), Cr(3)–P(6)–Cr(4) 132.7(2), P(1)–Cr(3)–P(6) 76.77–(14), P(2)–Cr(4)–P(6) 76.53(13), Cr(3)–P(1)–P(2) 112.8–(2), Cr(4)–P(2)–P(1) 118.1(2).

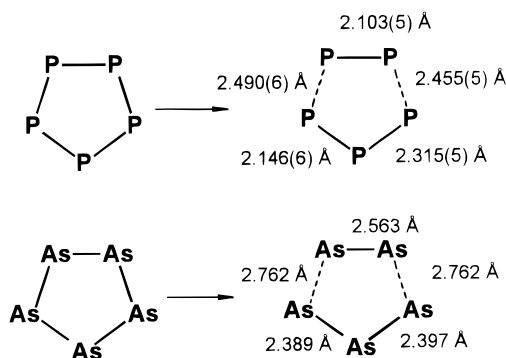


Figure 4. Details of the distortion of the cyclo-E₅ middle decks in **4** (above) and in [(CpMo)₂(μ,η⁵-As₅)] (below).

P₅)⁺ 16 but was found in [(CpMo)₂(μ,η^{4.4:1:1}-As₅)]¹⁷ (Figure 4). These compounds are 27 VE complexes according to the triple-decker formalism.¹⁸ By applying the polyhedral skeletal electron pair theory¹⁹ for a closo-delta-hedron containing five main groups and two transition metal vertexes, 50 skeletal electrons are needed, whereas in **4** a total of 47 electrons are found. Independent theoretical calculations of these systems reveal²⁰ that the distortion of the As₅ ring of the latter complex is the result of the first- and second-order Jahn–Teller distortion of the degenerate HOMOs, combined with a shortening of the metal–metal distance. In accordance with this, **4** reveals a Cr–Cr bond of 2.663(3) Å, significantly shortened in comparison to those found for [(CpCr)₂(η^{5.5}-P₅)] (2.738(1) Å)²⁷ and [(Cp*Cr)₂(η^{5.5}-P₅)]⁺ (3.185(1) Å).¹⁶ Furthermore, a slight increase in the P–P bond lengths is found if the P atoms of the cyclo-P₅ ring additionally coordinate to one or two metal fragments.

(16) Hughes, A. K.; Murphy, V. J.; O'Hare, D. *J. Chem. Soc., Chem. Commun.* **1994**, 163.

(17) Rheingold, A. L.; Foley, M. J.; Sullivan, P. J. *J. Am. Chem. Soc.* **1982**, *104*, 4727.

(18) Lauer, J. W.; Elian, M.; Summerville, R. H.; Hoffmann, R. *J. Am. Chem. Soc.* **1976**, *98*, 3219.

(19) (a) Mingos, D. M. P. *Acc. Chem. Res.* **1984**, *17*, 311. (b) Wade, K. *Adv. Inorg. Chem. Radiochem.* **1976**, *18*, 1.

(20) (a) Tremel, W.; Hoffmann, R.; Kertesz, M. *J. Am. Chem. Soc.* **1989**, *111*, 2030. (b) Jemmis, E. D.; Reddy, A. C. *Organometallics* **1988**, *7*, 1561.

(21) Goh, L. Y.; Wong, R. C. S.; Chu, C. K.; Hambley, T. W. *J. Chem. Soc., Dalton Trans.* **1990**, 977.

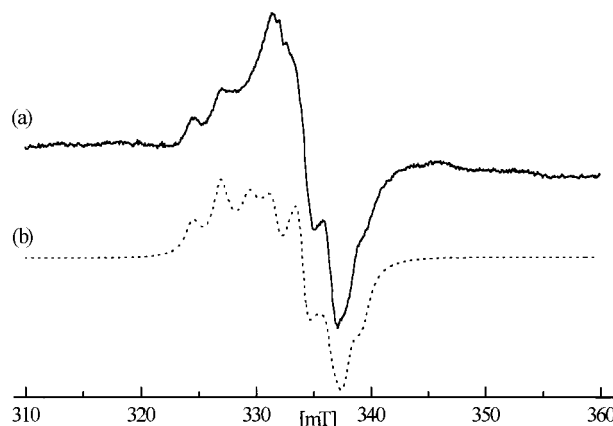


Figure 5. Experimental (a) and simulated (b) X-band EPR spectrum of **4** in toluene at $T = 130$ K.

Table 1. EPR^a Parameters of **4**

	g		A^P
g_1	1.998	A_1^P	15.5
g_2	2.019	A_2^P	21.7
g_3	2.063	A_3^P	23.6
g_{av}^b	2.027	A_{av}^P	20.3

^a Experimental error: $g_i \pm 0.003$; $A^P \pm 1.0$. Hyperfine couplings are given in 10^{-4} cm⁻¹. ^b $g_{av} = (g_1 + g_2 + g_3)/3$; $A_{av}^P = (A_1^P + A_2^P + A_3^P)/3$.

Such examples are found in [(Cp*Fe)(μ,η^{5.2}-P₅){Ir(CO)-Cp*}]^{4c} and [(Cp*Fe)(μ,η^{5.2:2:1}-P₅){Co(CO)Cp''}{Co₂Cp''-(μ-CO)}]^{4d} (Cp^x = η⁵-C₅Me₄Et; Cp'' = η⁵-C₅H₃tBu-1,3) where the corresponding elongated P–P bonds are 2.36 and 2.35 Å, respectively.

The experimental EPR spectrum of a frozen toluene solution of **4** is shown in Figure 5a. It can be described by a rhombic-symmetric spin Hamiltonian (eq 3) with

$$H_{sp} = \mu_B \cdot \mathbf{g} \cdot \mathbf{B}_0 \cdot \mathbf{S} + \sum_{i=1}^2 \mathbf{S} \cdot \mathbf{A}^{P_i} \cdot \mathbf{I}^{P_i} \quad (3)$$

an effective electron spin $S = 1/2$ and a hyperfine interaction with two magnetically equivalent ³¹P nuclei (second term in eq 3); all symbols have their usual meaning. Due to the small g anisotropy, the signals belonging to the three g tensor regions are considerably overlapped.

A satisfying simulation of the spectrum could be reached with the principal values of the tensors g and A^P (two ³¹P nuclei) given in Table 1 and is shown in Figure 5b for comparison.

Hyperfine interactions with other ³¹P nuclei of the compound are smaller than 4×10^{-4} cm⁻¹ and are not observed as a result of the experimental line widths. Their presence, however, is indicated by the small splittings seen on the low-field line of the g_2 region at 331 mT, which has the smallest line width of the spectrum. Also, ⁵³Cr hyperfine satellites (⁵³Cr: nuclear spin $I^{Cr} = 3/2$) were not observed. Considering the small natural abundance of ⁵³Cr (only 9.50%), the detection of the small satellites requires a very good signal/noise ratio, which could not be reached by our investigations.

The ³¹P hyperfine parameters can be used to estimate the spin density on these nuclei.^{22,23} For this, the

(22) Kirmse, R.; Stach, J. *ESR-Spektroskopie-Anwendungen in der Chemie*; Akademie-Verlag: Berlin, 1985; p 86–95.

Table 2. Crystallographic Data for 2–4

	2	3	4·C ₇ H ₈
formula	C ₁₄ H ₁₃ Cr ₂ O ₄ P	C ₁₄ H ₁₄ Cr ₂ O ₄ P ₂	C ₃₁ H ₂₉ Cr ₄ O ₄ P ₆
formula wt	380.21	412.18	859.36
cryst size, mm	0.75 × 0.27 × 0.15	0.19 × 0.11 × 0.08	0.08 × 0.02 × 0.02
T, K	200(2)	200(2)	200(1)
space group	orthorhombic	monoclinic	monoclinic
cryst syst	<i>Pccn</i>	<i>P2₁/n</i>	<i>P2₁/n</i>
a, Å	7.252(2)	14.156(3)	10.077(2)
b, Å	16.144(3)	23.050(5)	14.895(3)
c, Å	12.733(3)	15.818(3)	22.571(5)
β, deg	90.0	109.54(3)	97.68(3)
V, Å ³	1490.7(5)	4864(2)	3357.4(12)
Z	4	12	4
d _c , g/cm ³	1.694	1.689	1.700
μ _c , cm ⁻¹	1.575	1.549	1.583
F(000)	768	2496	1732
radiation (λ, Å)	0.710 73	0.710 73	0.710 73
diffractometer	STOE STADI IV	STOE IPDS	STOE IPDS
2θ range, deg	5.04 ≤ 2θ ≤ 55.0	4.46 ≤ 2θ ≤ 52.02	4.56 ≤ 2θ ≤ 41.64
hkl range	0 ≤ h ≤ 9, -20 ≤ k ≤ 0, -16 ≤ l ≤ 16	-17 ≤ h ≤ 12, -27 ≤ k ≤ 28, -17 ≤ l ≤ 19	-10 ≤ h ≤ 8, -14 ≤ k ≤ 14, -20 ≤ l ≤ 22
reflections collected	3290	19 339	7920
independent reflections with I > 2σ(I)	1507 (R _{int} = 0.0292)	6291 (R _{int} = 0.0557)	1672 (R _{int} = 0.1303)
data/restraints/parameters	1721/0/102	9291/0/673	3374/0/408
goodness-of-fit on F ²	1.102	1.033	0.853
R ₁ , ^a wR ₂ ^b (I > 2σ(I))	0.0313, 0.0785	0.0536, 0.1294	0.0524, 0.0685
R ₁ , ^a wR ₂ ^b (all data)	0.0398, 0.0908	0.0873, 0.1500	0.1397, 0.0879
largest diff peak, hole, e/Å ³	0.314, -0.595	0.501, -0.564	0.537, -0.393

^a $R = \sum |F_0| - |F_c| / \sum |F_0|$. ^b $wR_2 = [\sum \omega(F_0^2 - F_c^2)^2] / [\sum (F_0^2)^2]^{1/2}$. $c \omega^{-1} = \sigma^2(F_0^2) + (aP)^2 + bP$; $P = [F_0^2 + 2F_c^2]/3$.

isotropic part A_{av}^P and the dipolar part b^P of the ³¹P coupling are needed. Because the ³¹P hyperfine tensor is nearly axial-symmetric, A_2^P and A_3^P can be averaged to $A_{\perp}^P = 22.6 \times 10^{-4} \text{ cm}^{-1}$. With the relation $b = A_{\perp}^P - A_{av}^P$, the dipolar part is estimated to be $b = 2.4 \times 10^{-4} \text{ cm}^{-1}$. The spin densities $(c_{s,p}^P)^2$ can then be obtained by using eqs 4a and 4b where s and p represent the

$$(c_s^P)^2 = A_{av}^P / A_{av, \text{exp}}^P \quad (4a)$$

$$(c_p^P)^2 = b^P / b_{\text{exp}}^P \quad (4b)$$

atomic orbitals. Using the values $A_{av, \text{th}}^P = 4438.4 \times 10^{-4} \text{ cm}^{-1}$ and $b_{\text{th}}^P = 122.3 \times 10^{-4} \text{ cm}^{-1}$ calculated by Morton and Preston²³ and eqs 4a and 4b, the following spin densities per ³¹P nucleus are calculated: $(c_s^P)^2 = 0.5\%$ and $(c_p^P)^2 = 2.0\%$, yielding a complete spin density $\alpha^2 = (c_s^P)^2 + (c_p^P)^2 = 2.5\%$ per P atom. Thus 5.0% of the overall spin density is located on the two P atoms observed in the spectra. Because no ³¹P coupling is resolved for the other P nuclei of the complex, the main part of the spin density can be assumed to be localized in the central Cr₄P₂ unit.

Conclusions

The reaction of [$\{\text{CpCr}(\text{CO})_2\}_2(\mu, \eta^2\text{-P}_2)$] (**1**) with superhydride yields novel PH₂-containing products. Although the initial aim of synthesizing a dianionic starting material to generate novel metal-bridged oligomers and polymers was not achieved, reaction products **2** and **3** can be used themselves as starting materials for those purposes. These investigations are in progress. The formation of the complex **4**, which consists of a distorted cyclo-P₅ middle deck, reveals the strong tendency of Cr complexes to form triple-decker sandwich complexes with P_n ligands.

Experimental Section

General. All reactions and manipulations were performed under an atmosphere of dry argon using standard Schlenk techniques. Solvents were dried and distilled under an argon atmosphere prior to use: toluene and THF over Na/benzophenone, hexane over LiAlH₄, and dichloromethane over P₂O₅. [$\{\text{CpCr}(\text{CO})_2\}_2(\mu, \eta^2\text{-P}_2)$] was prepared according to a modified literature method.⁶ NMR spectra were recorded on a Bruker AC 250 (¹H, 250.133 MHz; ¹³C, 62.896 MHz; ³¹P, 101.256 MHz; standard ¹H and ¹³C, Me₄Si, ³¹P, 85% H₃PO₄). IR spectra were measured on a Bruker IFS 28 FT-IR spectrometer, and mass spectra were obtained on a Finnigan MAT 711 spectrometer at 70 eV. Satisfactory elemental analyses were obtained for **2–4**, which were performed on a Elementar Vario EL of the Institute of Inorganic Chemistry of the University of Karlsruhe.

Reaction of [$\{\text{CpCr}(\text{CO})_2\}_2(\mu, \eta^2\text{-P}_2)$] with LiBET₃H. A solution of [$\{\text{CpCr}(\text{CO})_2\}_2(\mu, \eta^2\text{-P}_2)$] (**1**) (0.5 g, 1.22 mmol) in THF at -78 °C was treated with 2 equiv of LiBET₃H (2.5 mL, 2.4 mmol). After the mixture was stirred for 20 min at -78 °C, the solution color changed from magenta to reddish brown. The reaction mixture was warmed slowly to room temperature, and it was stirred for a further 3 h. The solvent was removed in vacuo. Chromatographic separation on a silica gel column (35 cm × 2.5 cm) with *n*-hexane/CH₂Cl₂ (2:1) gives a green fraction of [$\{\text{CpCr}(\text{CO})_2\}_2(\mu\text{-PH}_2)(\mu\text{-H})$] (**2**) (0.15 g, 32% isolated yield after recrystallization from toluene) followed by a small magenta-colored fraction containing unreacted [$\{\text{CpCr}(\text{CO})_2\}_2(\mu, \eta^2\text{-P}_2)$] (**1**). With *n*-hexane/CH₂Cl₂ (1:1) an orange band is eluted, from which crystallized a mixture of orange [$\{\text{CpCr}(\text{CO})_2\}_2(\mu\text{-PH}_2)_2$] (**3**) (major amount) and a dark brown [$\{\text{CpCr}(\text{CO})_2\}_2(\mu\text{-PH})\}\{\text{CpCr}(\text{CO})_2(\mu, \eta^5\text{-P}_5)\}$] (**4**) (minor amount, 0.1 g total). The crystals were selected under a microscope in a glovebox.

Data for 2. IR [toluene, ν(CO)/cm⁻¹]: 1935 vs, 1881 s. ¹H NMR (C₆D₆): δ 4.03 (s, 10 H, C₅H₅), 5.07 (dd, 2 H, ¹J_{HP} 337 Hz, PH₂), -14.4 (d, 1 H, ²J_{HP} 75 Hz, CrHCr). ¹³C NMR (C₆D₆): δ 87.9 (C₅H₅), 233.1 (s, CO), 246.7 (d, ²J_{CP} 74 Hz, CO); ³¹P-{¹H} NMR (C₆D₆): δ 109.7 (s, PH₂). ³¹P NMR (C₆D₆): δ 110.5 (dt, ¹J_{PH} = 337, ²J_{PH} = 75 Hz, PH₂). EI-MS (70 eV, 50 °C): 380 (15) [M⁺]; 352 (1) [M⁺ - CO]; 324 (6) [M⁺ - 2CO]; 296

(23) Morton, J. R.; Preston, K. F. *J. Magn. Reson.* **1978**, *30*, 577.

(23) [M⁺ - 3CO]; 266 (61) [Cp₂Cr₂PH]; 182 (100) [Cp₂Cr]; 117 (18) [CpCr]. **Data for 3.** IR [toluene, $\nu(\text{CO})/\text{cm}^{-1}$]: 1932 vs, 1874 s. ³¹P{¹H} NMR (C₆D₆): δ -147.2 (s, PH₂). ³¹P NMR (C₆D₆): δ -147.2 (m, ¹J_{PH} = 177, ³J_{PH} = 117 Hz, PH₂). EI-MS (70 eV, 180 °C): 413 (5) [M + 1]; 356 (3) [M⁺ - 2CO]; 328 (1) [M⁺ - 3CO]; 296 (1.5) [Cp₂Cr₂P₂]; 267 (5) [Cp₂Cr₂PH₂]; 182 (15) [Cp₂Cr]; 117 (10) [CpCr]. **Data for 4.** EI-MS (70 eV, 180 °C): (%): 709 (2) [M⁺ - 2CO-H]; 683 (2) [M⁺ - 3CO]; 389 (5) [Cp₂Cr₂P₃]; 327 (2) [Cp₂Cr₂P₃]; 182 (15) [Cp₂Cr]; 117 (10) [CpCr].

X-ray Structure Determination and Details of Refinement. Data were collected on a STOE STADI IV (**2**, ω -scan mode) and a STOE IPDS (**3** and **4**) using Mo K α (λ = 0.710 69 Å) radiation with empirical absorption corrections for **2** ψ scans. Machine parameters, crystal data, and data collection parameters are summarized in Table 2. The structures were solved by direct methods using SHELXS-86,^{24a} full-matrix least-squares refinement on F^2 in SHELXL-93^{24b} with anisotropic displacement for non-H atoms, hydrogen atoms placed in idealized positions, and refined isotropically according to the riding model. The hydrogen atoms of the PH_{*n*} groups in **2**–**4**, as well as the bridging H atom of **2**, could be freely refined. For **3**, three independent molecules in the unit cell

were refined and were distinguished from each other by different folding angles of the Cr₂P₂ framework. The crystal quality of the toluene solvent of **4** was not very good. Every selected crystal displayed poor reflection at angles greater than 2θ ; therefore, the maximum 2θ limit of 42° were taken for the final refinements.

EPR Measurements. EPR spectra were recorded in the X-band ($\nu \approx 9.5$ GHz) on a BRUKER spectrometer of the type ESP 300E in the temperature range $295 \text{ K} \geq T \geq 130 \text{ K}$ using about 10^{-3} M solutions of **4**. The EPR parameters were obtained using a modified version of the computer program written by White and Belford.^{25,26}

Acknowledgment. The authors thank the Deutsche Forschungsgemeinschaft and the Fonds der Chemischen Industrie for financial support.

Supporting Information Available: Complete tables of atomic coordinates, H-atom parameters, bond distances, and anisotropic displacement parameters and fully labeled figures for **2**–**4**. This material is available free of charge via the Internet at <http://pubs.acs.org>.

OM990098U

(24) (a) Sheldrick, G. M. *SHELXS-86*; University of Göttingen, 1986.
(b) Sheldrick, G. M. *SHELXL-93*, University of Göttingen, 1993.

(25) White, L. K.; Belford, R. L. *J. Am. Chem. Soc.* **1976**, *98*, 4428.
(26) White, L. K. Dissertation, Urbana, IL, 1975; revised version written by K. Köhler and R. Böttcher, University of Leipzig, 1990.